Article:
Mohsenian, V., Padashpour, S. and Hajirasouliha, I. orcid.org/0000-0003-2597-8200 (2020) Seismic reliability analysis and estimation of multilevel response modification factor for steel diagrid structural systems. Journal of Building Engineering. 101168. ISSN 2352-7102

https://doi.org/10.1016/j.jobe.2019.101168

Seismic Reliability Analysis and Estimation of Multilevel Response Modification Factor for Steel Diagrid Structural Systems

Vahid Mohsenian[1], Saman Padashpour[2] and Iman Hajirasouliha[3*]

[1] *Department of Civil Engineering, University of Science and Culture, Tehran, Iran*

[2] *Department of Civil Engineering, K. N. Toosi University of Technology, Tehran, Iran*

[3] *Department of Civil and Structural Engineering, University of Sheffield, Sheffield, UK*

*Corresponding author; Email: i.hajirasouliha@sheffield.ac.uk

Abstract: Diagrid systems are emerging as one of the structurally efficient and architecturally aesthetic solutions for tall buildings. Despite the fact that such systems are increasingly used in modern construction, current literature lacks detailed information regarding their structural behaviour and seismic design parameters to ensure satisfactory performance under different earthquake intensity levels. This study aims to assess the seismic reliability of diagrid structural systems and develop more efficient performance-based design methodologies. Demand and supply response modification factors are calculated for 16, 24 and 32-storey buildings with diagrid structural systems using 65° diagrid angle and designed in compliance with current standards under a set of 12 spectrum compatible earthquakes. The results are then used to develop a novel multi-level response modification factor (R-Factor) for diagrid structural systems as a function of site seismicity and acceptable damage level. Subsequently, comprehensive seismic reliability analyses are conducted to assess the seismic performance of the selected structures under intensity levels corresponding to DBE and MCE hazard levels (earthquake scenarios with return periods of 475 and 2475 years, respectively). In general, results of this study demonstrate acceptable seismic performance and reliability of steel diagrid systems. It is shown that even using an R-Factor equal to 4 in the seismic design process could ensure that diagrid structures remain in a performance level higher than Life Safety (LS) for both DBE and MCE hazard levels. Multi-level response modification factors proposed in this study can be directly used in performance-based design of diagrid structures to satisfy different performance targets under any seismic hazard level.

Keywords: Diagrid Structural System; Demand Response Modification Factor; Supply Response Modification Factor; Seismic Reliability; Tall Buildings

1. Introduction

Congested urban areas as well as tendency to modernize architectural plans have driven the construction industry towards designing tall building structures. Selection of an efficient structural system to provide adequate lateral load-resisting capacity and withstand the seismic loads, is a challenging task as the building's height increases [1, 2]. While the importance of diagonal elements to resist against lateral loads has been fully proven since late 19th century, these elements were traditionally used in the building's core and interior spaces following poor insight towards the potential of facade architecture and ability to create beautiful views [3]. Accordingly, evolution of braced tubular systems and exposure of the diagonal elements led to emergence of a novel assembly called "diagrid system" comprised of diagonals with triangular schemes. This system offers the advantage of high lateral load resistance against wind and seismic loads, while it also provides more freedom for architectural design of irregular and complex shapes in tall buildings [4].

1.1. An overview on the applications of diagrid structural system

Diagrid structures are a particular form of space frames using the general form of tubular systems. As shown in Figure (1), the perimeter diagonal elements are utilised to keep the structure stable without the presence of any columns in the outer surfaces. On the contrary to the braced frames, in which the diagonal elements are designed to withstand the lateral loads, in case of diagrid systems the triangular modules provide the resistance under both gravity and lateral loads [3]. In such systems, the lateral loads are transferred through the diagonals placed in the perimeter of the structure, and therefore, a concrete core with considerable shear stiffness will not be required [5]. The dominant axial performance in the diagonals, can play an important role in minimizing the shear and flexural deformations of the system. Therefore, compared to conventional moment-resisting frame systems, using diagrid elements can considerably reduce the steel consumption.

Mele et al. [6] investigated the load resisting mechanism of diagrid buildings subjected to both gravity and wind loads. Subsequently, a simplified approach was adopted to estimate the member sizes of the triangular modules. Similarly, Moon [7] proposed design provisions to efficiently employ the diagrid system in complex and non-prismatic forms of tall buildings. The capabilities of the diagrid system to design sustainable high-rise buildings have been demonstrated by Asadi

and Adeli [8]. Asadi and Adeli [9] investigated the nonlinear seismic behaviour of steel diagrid structures in terms of fundamental period, lateral stiffness, inter-storey drift and sequence of plastic hinge formation. More recently, Asadi et al. [10] developed an integrated decision model for seismic resilience and sustainability assessment of diagrid systems.

Fig 1: An example of Diagrid Tube Structure: Swiss Re Building, London

By developing a framework for seismic performance assessment of diagrid buildings, Asadi et al. [11] demonstrated the substantial collapse capacity and lateral stiffness of this structural system. The results of their study indicated that the diagonals angle, building height, and incomplete diagrid modules can affect the seismic performance of diagrid buildings. In another relevant study, Lacidogna et al. [12] proposed a matrix-based method (MBM) for more efficient analysis of two-dimensional and three-dimensional diagrid systems. To optimize the geometry of diagrid systems, Zhang and Zhao [13] investigated the impact of variation in diagonals angle along the building's height on the lateral load capacity and material consumption, considering different height to width aspect ratios. Accordingly, they proposed critical aspect ratios to obtain the most desirable results. In another relevant study, Zhang et al. [14] concluded that if the height to width aspect ratio exceeds a critical value, a gradual change in diagonals angle leads to the

most desirable design in terms of material consumption. Furthermore, it was specified that if the height to width aspect ratio falls below the critical value, using a uniform angle for diagonals aids to achieve the best design solution. Moon et al. [3] found that, depending on the height and aspect ratio of diagrid structures, the optimal range of diagrids angle is generally from about 55° to 75°. Similarly, studies conducted by Kim and Lee [5] indicated that the diagrid structures with the brace angle between 60° to 70° generally provided the most efficient load resisting system under both lateral and gravity loads.

Montouri et al. [15] evaluated the adequacy of stiffness and strength-based methods for the design of diagrid structures and proposed a simple approach to quickly estimate the required size of the elements in diagrid systems. Similarly, Moon [16] study indicated that in case of diagrid structures with a constant diagonals angle, the optimal angle should be increased to achieve the desirable design aiming to reduce material consumption and lateral displacements. In this study, optimal angles ranged between 60 to 70 degrees were found to be suitable for a wide range of designs with various aspect ratios. It was also shown that for the aspect ratios greater than 7, in which flexural behaviour prevails, increasing the angle of diagonals from top to base level of the structure generally leads to a more economic design compared to the constant diagonals angle. In contrast, in the case of low aspect ratios (lower than 7), the design will be more economic if the diagonals angle is kept constant along the height of the structure. In another relevant study, the seismic performance of diagrid structural systems was evaluated by Kim and Lee [5]. In this study, the optimal angle for diagonals was also reported to be between 60 to 70 degrees. In addition, it was specified that by increasing the diagonals angle, the lateral strength is reduced while the shear lag effects are intensified. It was also shown that diagrid buildings with circular plans generally have better performance compared to those with rectangular shapes.

In more recent studies, Tomei et al. [17] used genetic algorithm (GA) approach to optimize regular and irregular diagrid systems with complex geometries aiming to minimize the required structural weight. Asadi and Adeli [18] also carried out studies to evaluate the seismic performance parameters for low to mid-rise diagrid structures. In their studies, an R-factor in the range of 4 to 5 was recommended for typical steel diagrid frames with 8 to 30 storeys. For low-rise steel diagrid systems (under 8 storeys), an R factor in the range of 3.5 to 4 was found to be suitable. In another study, Heshmati and Aghakouchak [19] employed the method proposed by FEMA P695 [20] to estimate the R factor for diagrid structures and found that the value of 4.5

generally leads to satisfactory results. In addition, it was observed that as the angle of the peripheral diagonal elements increases, the overstrength and the collapse margin ratios decrease while the ductility of the system increases.

It should be noted that, considering the special geometry and shape of diagrid systems, construction of diagonals' connections can be challenging [21]. A few experimental studies have been performed to understand the behaviour of such connections under reversed lateral loads [22-24]. Previous studies also indicated that if diagrid systems are designed in accordance with current standards, they generally exhibit a better performance in terms of shear lag and storey drifts compared to other types of tubular structural systems [25]. While there are some studies conducted on the analysis of progressive collapse in such systems [26, 27], less information is available on the seismic reliability and design parameters suitable for performance-based design procedures.

1.2. Research Significance and Novelty

Although diagrid systems are increasingly used in tall buildings, current design codes generally do not account them as an independent structural system. As a result, there is no agreement on the suitable behaviour factor for these systems to satisfy required performance targets under Design Basis Earthquake (DBE) and Maximum Considered Earthquake (MCE) hazard levels (i.e. earthquake scenario with return period equal to 475 and 2475 years, respectively). To address this issue, through reliability studies on a wide range of nonlinear models, this study aims to assess the seismic performance of diagrid systems and subsequently provide a novel multi-level response modification factor based on the site seismicity and target performance levels. Unlike most conventional methods, to improve the accuracy and reliability of the results, local damage criteria (instead of global damage criteria) are utilized to determine the performance level and supply response modification factors. The proposed response modification factors can be efficiently utilized in the performance-based design of diagrid systems is seismic regions to provide more reliable design solutions.

2. Numerical Models' Specifications

Buildings with plan views and façade geometry shown in Figure (2), have been numerically studied. To investigate the effect of height on the structural responses of diagrid systems, 16, 24 and 32 storey buildings with the same plan are considered. The models are respectively

comprised of 4, 6 and 8 diamond-shaped modules (each 4 storey forms a module). As it can be seen in Figure (2), in each model and along the height of a module, the plan is variable. Considering the height of the storeys (3.3 m), all the three models are classified as tall buildings (height greater than 50 m) according to the Iranian Code of Practice for Seismic Design of Buildings (Standard No. 2800) [28]. It should be noted that this standard is mainly based on ASCE/SEI 7-10 [29]. The site of study is assumed to be of high seismicity with soil type "II" (375 m/s ≤Vs≤750 m/s) based on the classification specified by Standard No. 2800 [22]. The soil type "II" in the Iranian code [28] is equivalent to site class C in ASCE/SEI 7-10 [29], which represents a very dense soil or soft rock.

In this study, the buildings were designed based on AISC 360-10 [30] using ETABS Software [31]. For the preliminary design process, the response modification factor was considered to be 3.5 [32, 33]. The value of live and dead loads applied to the storeys were selected to be 4 and 2.5 kN/m^2, respectively. In the developed models, the angle of diagonals with horizontal direction (θ) was equal to 65°, which is in the optimum range of diagrid angles proposed in previous research studies [3, 5, 16]. While this parameter is generally obtained based on the height-to-width aspect ratio of the building, it can considerably influence the seismic response and load bearing resistance of the diagrid system [5, 14, 16]. The beams located in building's perimeter as well as the frame elements in the central core were designed for both gravity and lateral seismic loads. It should be noted that while the connections at both ends of floor beams are hinged, these elements can still contribute to the lateral load-carrying capacity and ductility of diagrid systems [9].

To avoid local and global buckling in the diagonal members, they were designed as box sections with maximum width to thickness ratio of $0.55\sqrt{E/Fy}$, in accordance with ANSI/AISC 341-10 [34] requirements for highly ductile compression members. E and Fy represent the Young modulus and yield stress of steel material, respectively. To control the brittle fracture of the members under extreme earthquake load events, the overstrength factor (Ω_0) was assumed to be 1.5. The specifications of the diagonal members designed for each module are illustrated in Figure (2). In this study, beams and diagonals were assumed to be made of ST37 and ST52 grade steel, respectively [35].

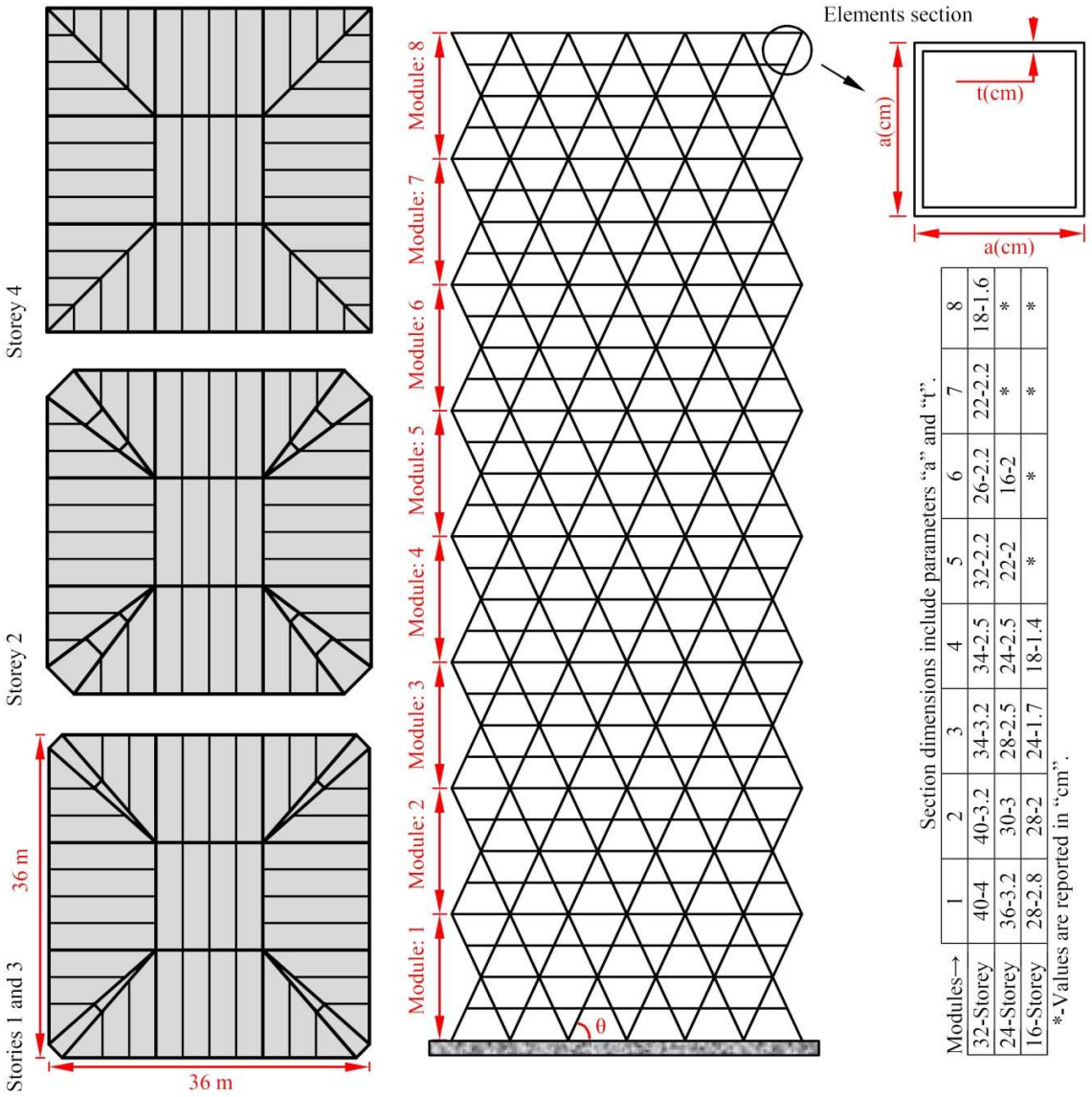

Section dimensions include parameters "a" and "t".

Modules→	1	2	3	4	5	6	7	8
32-Storey	40-4	40-3.2	34-3.2	34-2.5	32-2.2	26-2.2	22-2.2	18-1.6
24-Storey	36-3.2	30-3	28-2.5	24-2.5	22-2	16-2	*	*
16-Storey	28-2.8	28-2	24-1.7	18-1.4	*	*	*	*

*-Values are reported in "cm".

Fig (2): Plan variations in modules, façade and geometric specifications of diagonals in the studied diagrid buildings

3. Nonlinear Modelling and Determination of Strength and Deformation Parameters

PERFORM-3D Software [36] was utilized to carry out nonlinear analyses on the designed models. Due to the higher stiffness of the diagonal elements, it was assumed that the beam elements do not exhibit buckling under compressive axial loads imposed by the earthquake excitations [19]. As a result, standard sections with linear behaviour were used to model the beams elements. For modelling of the diagonal members, inelastic fibre sections with spread plasticity were utilized. Since most studies regarding diagrid structural systems have emphasized

the dominant axial behaviour of diagonal elements [6], the acceptance criteria for these elements in nonlinear range was based on the general relation of load-displacement as depicted in Figure (3). For the element in which energy absorption is accomplished via formation of axial hinges, axial deformations in the expected buckling load (Δ_c) and the tensile force corresponding to yield limit (Δ_t) were chosen as the main control criteria [37].

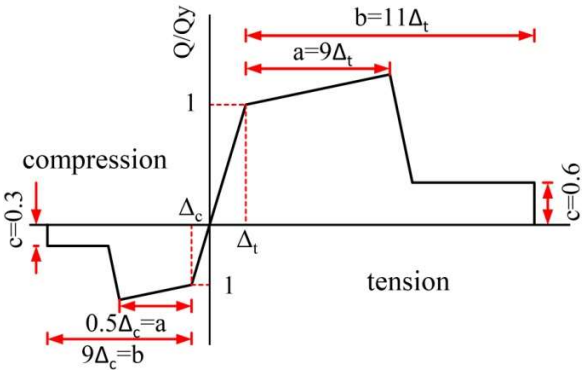

Fig (3): Generalized Load-Displacement Curve for steel elements in accordance to [37]

The axial deflections are calculated by using Equations (1) and (2), while the expected strength of diagonals under tension (T_{CE}) and the lower bound of strength under compression (P_{CL}) are considered as the member forces. In these equations, L is the free length of diagonal member, and E and A represent the modulus of elasticity and the area of element section, respectively. To obtain the yield state and characteristics of diagonal member, load-displacement parameters a, b and c (see Figure (3)) have been chosen based on the acceptance criteria in nonlinear methods for steel elements in accordance to ASCE/SEI41-17 [37].

$$\Delta_t = \frac{T_{CE} \cdot L}{EA} \qquad (1)$$

$$\Delta_c = \frac{P_{CL} \cdot L}{EA} \qquad (2)$$

Some of the other simplifying assumptions made herein include rigid diaphragm for floors, rigidity of connections at base level and intersection of diagonals, and neglecting the foundation uplift.

4. Analysis of the Natural Frequencies

To analyse the buildings, the upper limit of gravity load effects is considered using the following load combination to take into account the most critical condition in terms of buckling of diagonal members [37]:

$$Q_G = 1.1[Q_D + Q_L] \quad (3)$$

where "Q_D" and "Q_L" represent the dead and live loads, respectively.

Vibration periods and factors of effective translational mass in the first 10 modes of vibration are presented in Table (1). As expected, the results of Eigenvalue analysis indicate that by increasing the building's height, in addition to an increase in the period of vibration modes, the factor of effective translational mass in the first mode is also reduced.

Table 1: Effective translational mass and vibration periods of different modes

Models→	16-Storey		24-Storey		32-Storey	
Mode No.	M (%)	T (sec)	M (%)	T (sec)	M (%)	T (sec)
1	64.9	1.02	62.1	1.42	59.8	2.03
2	3.69	0.567	1.57	0.623	1.00	0.585
3	3.61	0.358	10.7	0.421	13.34	0.502
4	9.50	0.292	1.98	0.366	1.17	0.361
5	4.85	0.254	1.77	0.299	2.70	0.291
6	3.45	0.216	2.3	0.253	3.21	0.256
7	0	0.188	7.84	0.222	1.20	0.224
8	1.72	0.174	2.65	0.199	3.97	0.197
9	8.30	0.141	0	0.190	8.16	0.182
10	0	0.098	1.2	0.172	0.60	0.178

It should be noted that since the factors of mass contribution of all models in the first translational modes are less than 75% and the vibration periods of the 1st modes are greater than 1s, it will be inadequate to analyse the buildings using push over analyses with a simplified triangular distribution for seismic loads along the building's height, in which the effects of higher modes are excluded. Therefore, in this study time-history analyses are used to assess the seismic response of diagrid systems as will be explained in the following section.

5. Time-History Analysis

To match the applied ground motions with site seismicity, in this study artificial records corresponding to the selected code-based spectrum, in accordance with the Iranian code 2800 [29], were utilized. To this end, 12 earthquake records were artificially extracted by modifying

the natural accelerograms making use of wavelet transform method from the site demand spectrum [38]. In wavelet transform approach, through transferring the selected accelerogram to the wavelet domain and modification of its detail functions with ratio of target to response spectrum of this motion and return to the time domain, a motion with a spectrum closer to the target spectrum is generated. This process is repeatedly conducted until an adequate level of accuracy is achieved. In this study, the main component of the original earthquakes used to produce the artificial records are listed in Table (2). The selected records are all far-field records obtained from the PEER database [39], and designated in a way to fully reflect the selected site soil condition (375 m/s $\leq$Vs$\leq$750 m/s). The peak ground acceleration (PGA) of the generated artificial records (or demand earthquakes) is close to that of the DBE (PGA=0.35g). In Figure (4), the spectra of these accelerograms are compared with the demand spectrum provided in accordance with the soil type and DBE hazard level for the selected site (see Section 2). In this study, the earthquakes corresponding to MCE hazard level (return period of 2475 years) were obtained by scaling the generated artificial records by factor of 1.5 (i.e. PGA equal to 0.55g).

Table 2: Earthquakes selected to generate artificial accelerograms and seismic reliability analysis

No.	Earthquake & Year	Station	M_W	R[a](km)	PGA(g)
1	Cape Mendocino, 1992	Eureka – Myrtle & West	7.1	44.60	0.1782
2	Northridge, 1994	Hollywood – Willoughby Ave	6.7	25.70	0.2455
3	Northridge, 1994	Lake Hughes #4B - Camp Mend	6.7	32.30	0.0629
4	Cape Mendocino, 1992	Fortuna – Fortuna Blvd	7.1	23.60	0.1161
5	Northridge, 1994	Big Tujunga, Angeles Nat F	6.7	24.00	0.2451
6	Landers, 1992	Barstow	7.4	36.10	0.1352
7	San Fernando, 1971	Pasadena – CIT Athenaeum	6.6	31.70	0.1103
8	Hector Mine, 1999	Hector	7.1	26.50	0.3368
9	Kobe, 1995	Nishi-Akashi	6.9	8.700	0.5093
10	Friuli, Italy, 1976	Tolmezzo	6.5	20.20	0.4169
11	Kocaeli (Turkey), 1999	Arcelik	7.5	53.70	0.2188
12	Chi Chi(Taiwan), 1999	TCU045	7.6	77.50	0.5120

[a] Closest distance to fault rupture

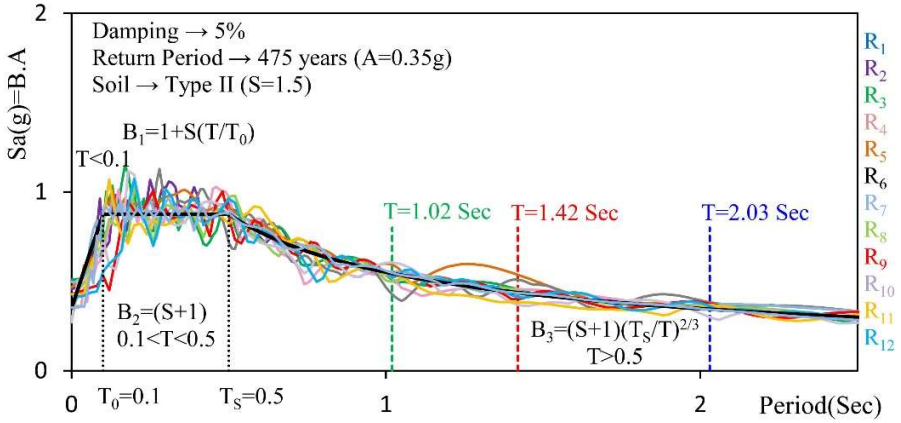

Fig (4): Comparison between the response spectrum of the developed artificial records (Ri) with the selected design-basis earthquake (DBE)

5.1. Structural Responses

Maximum storey drifts and shear forces developed under DBE and MCE hazard levels are obtained and their mean values are used to study the response of the systems (Figures (5) and (6)). According to Figures (5) and (6), the structural responses are sensitive to the intensity of input excitation. It can be noticed that under the selected level of intensity, maximum storey drifts in the last module of the three models, are considerably higher than the other storey levels, which is mainly due to the contribution of higher modes as discussed before.

In case of DBE hazard scenario, the maximum storey drifts in both elastic and inelastic models are coincident with each other. This implies that the structures remain elastic at this level of intensity. The results also show that the selection of deflection amplification factors (C_d) greater than 1 lacks rationale in this case as this factor is generally used for inelastic systems. The drift values at this intensity level are less than the allowable limit of 2% specified by the Iranian Code of Practice for Seismic Design of Buildings [28].

As expected, it can be seen in Figure (6) that by increasing the earthquake intensity level, the maximum storey shears also increase, especially at the lower levels of the structures. However, for all the three models, the maximum storey shears were always less than the design values. It can be also concluded from Figure (6) that the general procedure adopted in the preliminary design, including distribution of shear and lateral loads in the storeys, and control of brittle failure modes under amplified earthquakes as recommended by Iranian Code of Practice for Seismic Design of Buildings [28], have led to satisfactory results.

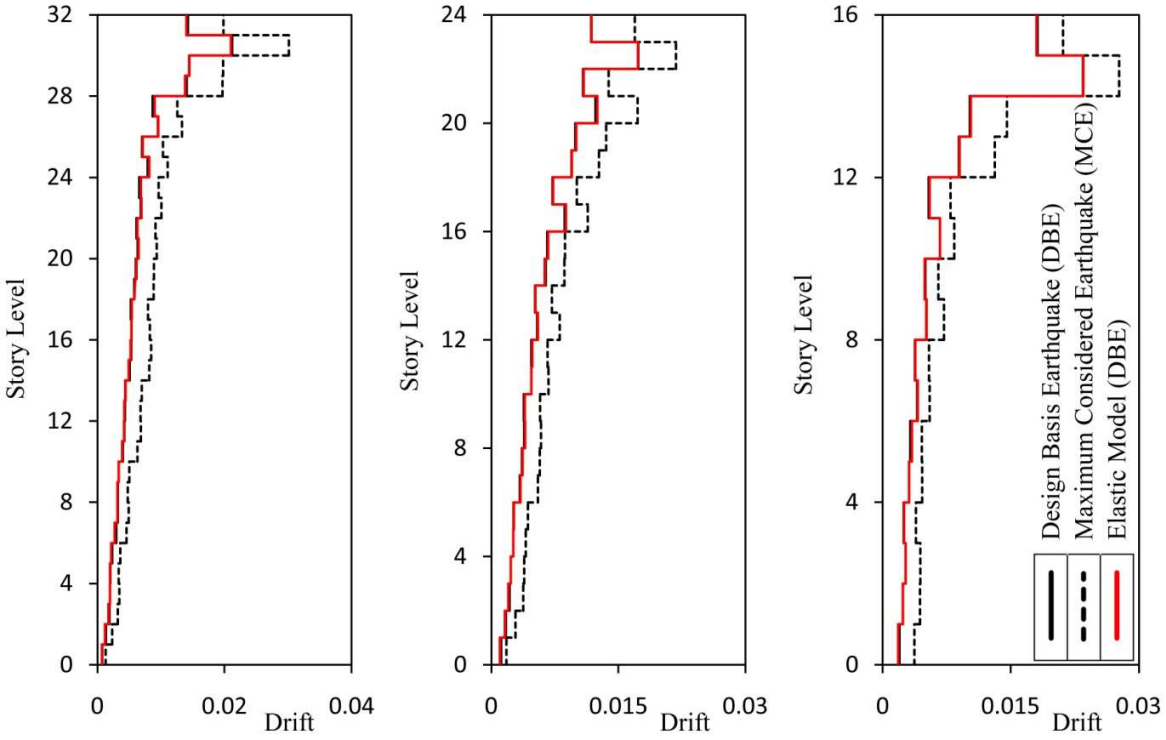

Fig (5): Mean values of maximum storey drifts

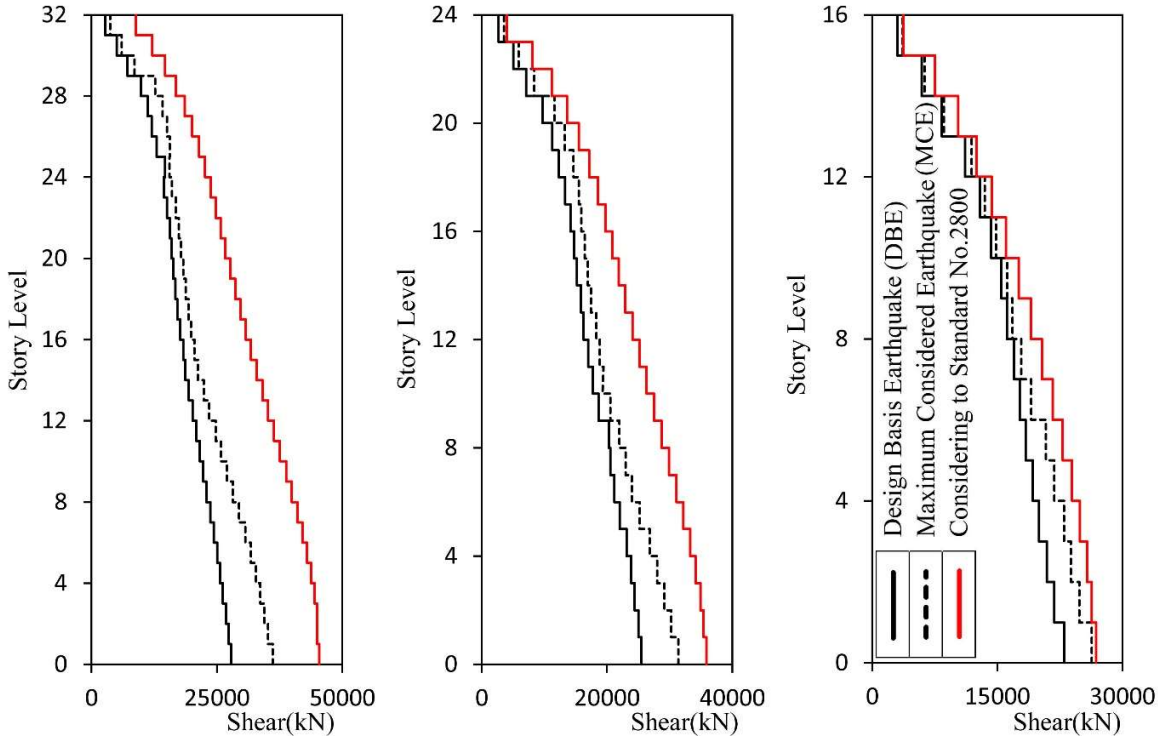

Fig (6): Mean values of maximum storey shears

5.2. Evaluation of Axial Strain Distribution

Figure (7) illustrates the location of damage initiation and its distribution mechanism along the buildings' height in the studied buildings. Strain contours for the elements after experiencing the intensity corresponding to MCE are also presented in this figure.

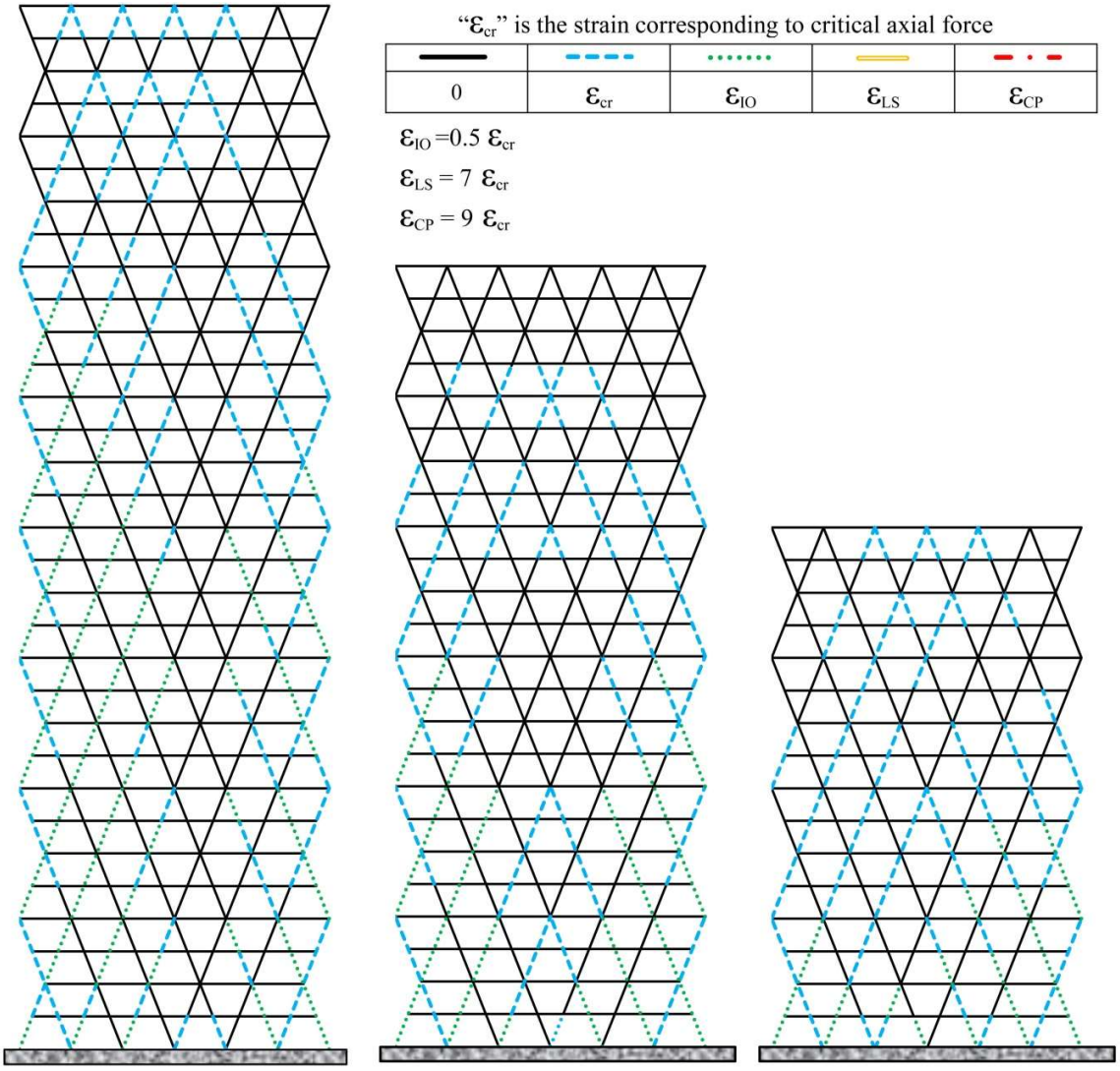

Fig (7): Strain distribution in diagonals under the MCE hazard level

It is of note that the limit strains of "ε_{IO}", "ε_{LS}" and "ε_{CP}" represent the performance levels of immediate occupancy (IO), life safety (LS) and collapse prevention (CP) [37]. Under DBE hazard scenario, the ratio of maximum axial strain in diagonal elements to the axial strains

corresponding to critical buckling load (ε_{cr}) in 16, 24 and 32-storey buildings were equal to 1.91, 2.06 and 1.79, respectively. Under MCE hazard level, these ratios changed to 3.85, 3.54 and 3.6, respectively. The accepted level of the above mentioned parameter for performance levels of life safety (LS) and collapse prevention (CP) are proposed to be respectively 7 and 9 [37]. This implies that under both hazard levels, the structures were in a performance level higher than life safety. The results indicated that the rate of variations in axial strain developed in the elements located in the first module (particularly first storey and peripheral elements), is greater than that of the other elements. Clearly, higher levels of damage are expected to develop in these elements.

5.3. Engineering Demand Parameter (EDP) Based Approach

In this approach, the engineering demand parameter is considered as a variable to determine the limit state of damages in the structure [40]. Accordingly, incremental dynamic analyses (IDAs) are conducted on the structures to obtain Engineering Demand Parameter (EDP) values. Peak Ground Acceleration (PGA) and maximum axial strain in diagonals are respectively adopted as Intensity Measure (IM) and Damage Measure (DM) parameters. It should be mentioned that compared to using the storey drift as a global damage index, the above mentioned measures (i.e. local damage indices) can better represent the actual damage in the systems, especially since current standards do not offer any provisions for the assessment of the buildings with diagrid systems. Using the EDP-approach can considerably reduce the computational costs required to obtain the reliability of the system for a specific performance target.

In what follows, for a certain value of intensity (IM= constant), the probability of reaching the limit states corresponding to different levels of damage have been determined. The steps to be taken are as follows: (i) Maximum values of structural response under each record scaled to a certain PGA are obtained; (ii) Assuming that the calculated values are of a normal distribution, a probability density function, f(x), is developed by computing mean (μ) and standard deviation (δ) parameters for the values obtained at this level of intensity as shown in Figure (8-a). In this figure, the area under the curve of probability density function from "$-\infty$" to the target damage level (i.e. "ε_{LS}", "ε_{CP}"), signifies the reliability of the system [41]. Figure (8-b) also shows the Cumulative Distribution Function (CDF) for DBE and MCE hazard levels for the studied diagrid systems.

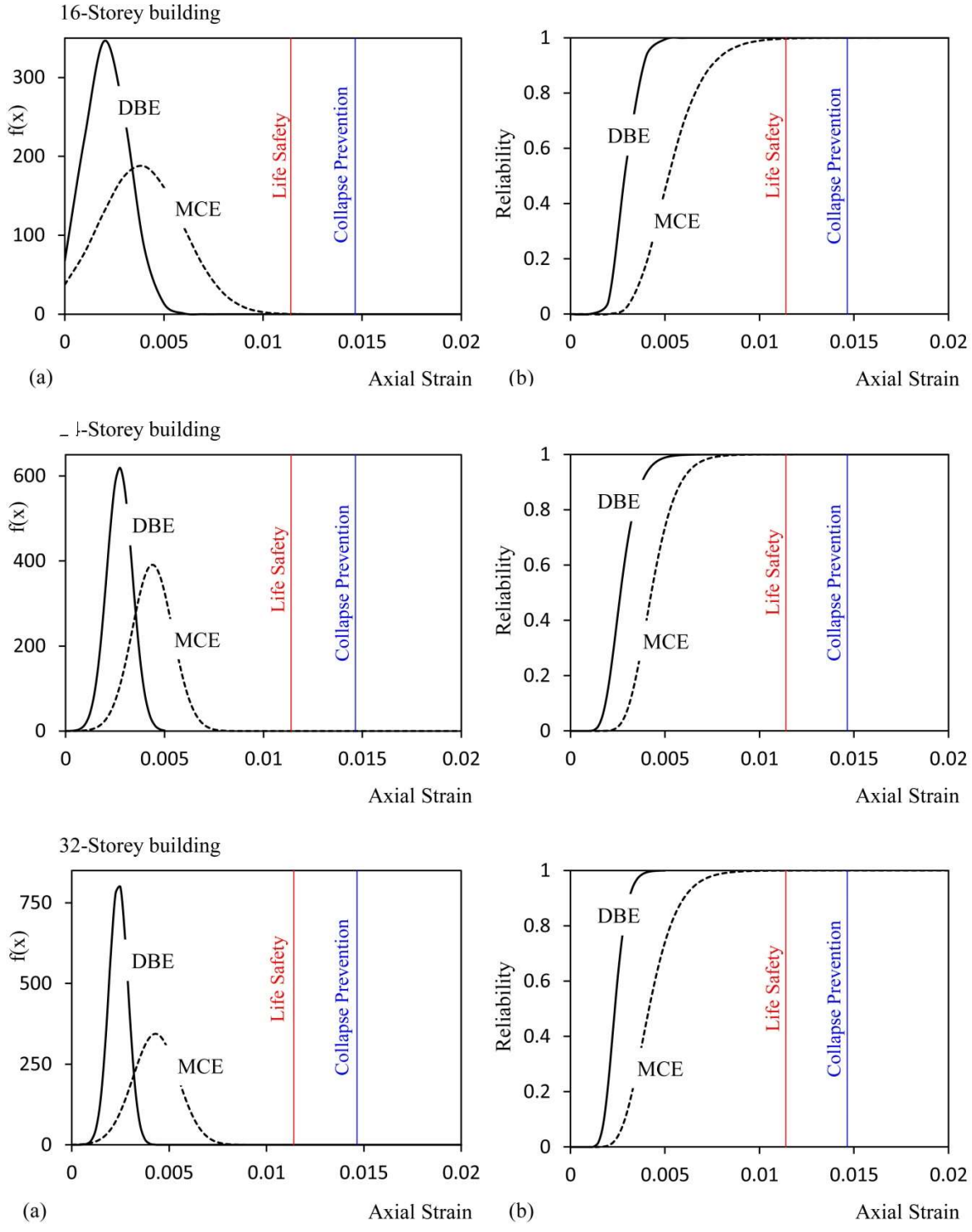

Fig (8): (a) Probability Density Functions (PDF) and (b) Cumulative Distribution Functions (CDF) of 16, 24 and 32-storey buildings for DBE and MCE hazard levels

For the studied structures, under the two hazard levels of DBE (PGA=0.35g) and MCE (PGA=0.55g), the probabilities are derived in compliance with the described process for different limit states in diagonals as presented in Table (3). The results show that at both levels of intensity, the reliability of diagonal elements for not exceeding the performance levels of life safety (LS) and collapse prevention (CP) is greater than 99%. In other words, under DBE and MCE hazard levels, all the studies structures are at performance levels higher than life safety. It is also shown that the three models have the same probabilities to reach various performance levels, and therefore, the overall reliability of the systems is not affected by the building's height. Moreover, as the intensity levels increase, the performance level of the structures is not remarkably affected, although the rate of dispersion in the results is signified. With reference to the results obtained herein, it is concluded that the studied diagrid structural systems possess a high seismic reliability, when R-Factor equal to 3.5 is used in the preliminary design process.

Table 3: Reliability values to reach different limit states under DBE and MCE hazard levels

Structures →	16-storey		24-storey		32-storey	
Hazard Levels →	DBE	MCE	DBE	MCE	DBE	MCE
$\varepsilon_{IO}=0.5\ \varepsilon_{cr}$	0	0	0	0	0	0
ε_{cr}	0.41	0	4.12	0	4.6	0.05
$\varepsilon_{LS}=7\ \varepsilon_{cr}$	100	99.72	99.99	99.99	100	99.97
$\varepsilon_{CP}=9\ \varepsilon_{cr}$	100	99.98	100	99.99	100	99.99

6. Estimation of Response Modification Factor

Based on the current literature, code-based (design), demand (displacement/ductility) and supply concepts are used to estimate response modification factors as described in what follows [41].

6.1. Code-Based Response Modification Factor (R_{Code})

The response modification factors provide by seismic design codes are generally based on engineering judgments, experiences and lessons learned during the past earthquakes. The main reason behind introducing the response modification factor by seismic design codes (R_{Code}) is to include the effects of ductility demand in conventional force-based design methods. However, many researchers have studied the limitations of using R_{Code} concluding that a more rigorous estimation is required to provide higher reliability in the methods and provisions prescribed by the codes [42, 43]. The values of R_{Code} in Standard No. 2800 [28] (and ASCE/SEI 7-10 [29]) are independent of the period of the building, and are presented based on the adopted structural

system and material type. Diagrid is relatively a newly-developed structural system, and therefore, there is not much information regarding its seismic performance in past earthquakes. Moreover, currently there is no specific code addressing the design issues of such systems. In this study, the response modification factor utilized for preliminary design was equal to 3.5, which is based on the value commonly selected by practitioners.

6.2. Demand Response Modification Factor, R_{Demand} (Displacement/Ductility)

The value of demand response modification factor depends on site seismicity as well as the physical and geometrical specifications of the building. Previous studies indicated that parameters like earthquake magnitude and focal depth do not considerably affect the R_{Demand} compared to the other parameters such as ductility, energy absorption, fundamental period, overstrength, redundancy, number of degrees of freedom and soil type [44-46].

Demand response modification factor, R_{Demand}, is generally defined based on Equation (4):

$$R_{Demand} = R_{\mu}^{MDOF} . \Omega_s . R_d \quad (4)$$

where R_{μ}^{MDOF} denotes the modification factor originated form ductility and dissipated energy caused by residual behaviour; Ω_s represents the overstrength factor which is used to consider the effect of redistribution of actions due to redundancy; and R_d is allowable stress factor defined as the ratio between the first significant yield and the design force levels. It should be noted that R_{Demand} can be also calculated by multiplying R_M (modification factor for number of degrees of freedom) and R_{μ}^{SDOF} (ductility factor of the equivalent single degree of freedom system) [47, 48]. However, in this study the demand response modification factors have been directly extracted from the actual multi-degree of freedom systems using the following steps:

First, capacity curve of the building is generated by means of dynamic pushover method. As shown in Figure (9-a), incremental dynamic analyses (IDA) are then conducted on the nonlinear model under the artificial records introduced in Section 5. In each analysis step, maximum values of base shear (V) and total drift (U), which is represented by the ratio of roof displacement (Δ) to overall building's height (H), are recorded. The obtained diagram using the average of the results for the spectrum compatible artificial records (R_1 to R_{12}) is defined as the dynamic capacity curve of the structure.

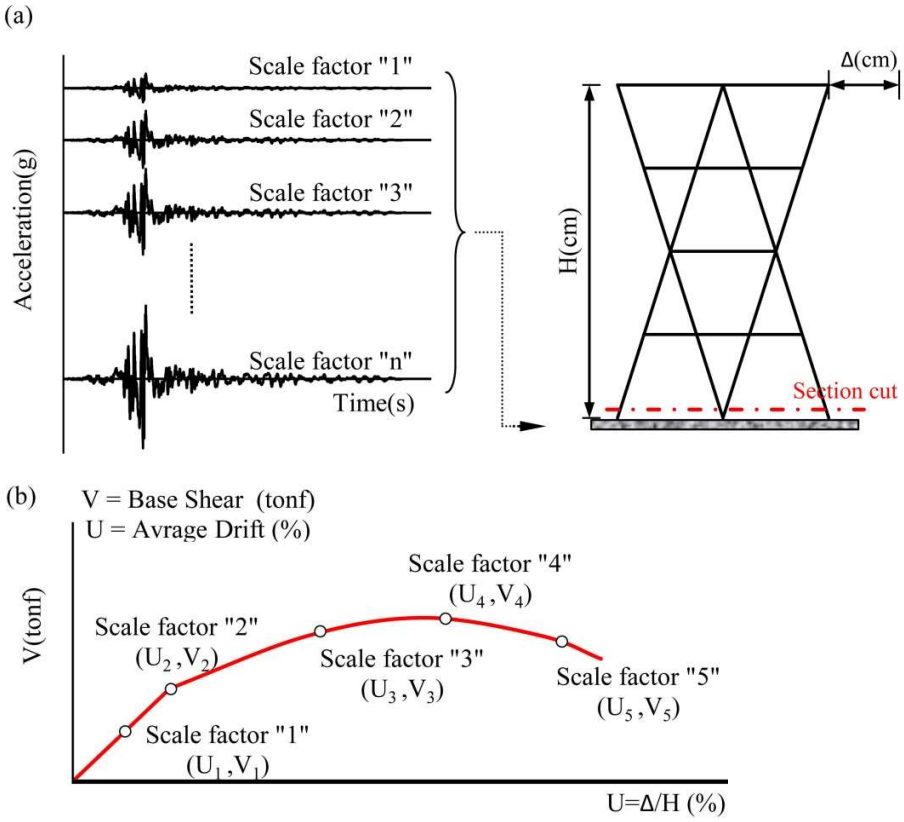

Fig (9): Schematic representation of generating Dynamic Capacity Curve: (a) Incremental Dynamic Analyses (IDA) on a diagrid system; (b) Average values of total drift (U) and base shear (V) corresponding to each scale factor

Assuming a linear behaviour for the structure, the resulted base shear is obtained through applying demand earthquakes to the structure, which is called elastic base shear (Ve). The design acclerograms are then applied to determine the maximum roof displacement by assuming a nonlinear behaviour for the system. This value represents the maximum drift corresponding to DBE hazard level (i.e. target drift), and is specified as a target on the capacity curve derived by dynamic pushover analysis. Subsequently, after bi-linearizing the response curve according to Figure (10), yield base shear (Vy) is calculate [37].

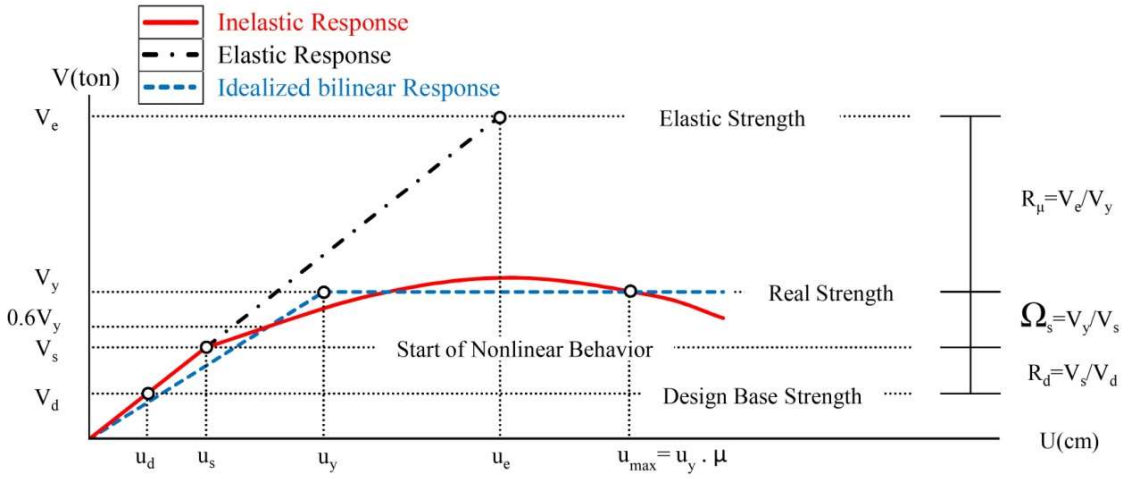

Fig (10): Bi-linearization of the capacity curve and the parameters used to calculate the Demand Response Modification Factor

The maximum intensity triggering the initiation of nonlinear behaviour can be simply obtained from the response resulted from the incremental dynamic analysis, and also based on the maximum axial strain developed in the diagonal members. The design base shear is then derived by dividing the multiplication of spectral acceleration obtained from the building's linear spectrum by its total weight, to code-based modification factor (here 3.5).

Derivation of the demand R factor according to Equation (4), ends by calculating the above mentioned parameters based on Equations 5 to 7 [49-51]. As an example, Tables (4) to (6) show the steps to calculate the demand R-factor for 16, 24 and 32-storey systems under the artificial accelerogram R_1 (see Figure 4). The mean values obtained from all accelerograms are introduced as Demand Response Modification Factor shown in Figure (11).

$$R_\mu = V_e / V_y \quad (5)$$

$$\Omega_s = V_y / V_s \quad (6)$$

$$R_d = V_s / V_d \quad (7)$$

6.3. Supply Response Modification Factor, R_{Supply} (Capacity)

This factor depends on the building's capacity to withstand nonlinear deformations and satisfy the predefined performance levels. The following algorithm can be used to derive the supply response modification factor based on the lateral strength of the structure [52]:

Incremental dynamic analysis (IDA) is conducted on the nonlinear structure under the earthquake records representing the site conditions. Subsequently, PGA factors corresponding to the target structural damage level are obtained. In this study, the PGA factors are calculated for the cases where maximum strain developed in diagonal members reaches the value corresponding to life safety (LS) and collapse prevention (CP) performance levels. This has resulted in two supply response modification factors R^1_{Supply} and R^2_{Supply} corresponding to LS and CP performance levels, respectively.

For the PGA levels obtained in the previous step, linear dynamic analysis is conducted and the base shear values are obtained from each analysis (Ve). A dynamic capacity curve is then generated for each accelerogram. Considering the target displacement corresponding to the damage levels taken in the first step, the capacity curve is bi-linearized in compliance with ASCE/SEI41-17 [37] proposed method. Based on the equivalent bilinear curve, the yield base shear (Vy) is calculate (see Figure 10). From this step onwards, the same steps and relations taken to obtain demand response modification factor, are adopted to calculate the supply factor. Tables (4) to (6) contain all steps and parameters required to calculate the supply response modification factor of the studied buildings. Herein, an acceleration corresponding to damage and a supply factor is derived for each accelerogram and similar to what explained earlier, the mean values for the 12 spectrum compatible artificial records (R_1 to R_{12}) are presented as Supply Response Modification Factor in Figure (11).

Table 4: Demand and Supply R-Factors for the 16-Storey building under an artificial spectrum compatible accelerogram (R_1)

Shear values are reported in (kN)	R Code	R Demand	R^1Supply	R^2Supply
Maximum ground acceleration (g)	0.35	0.35	1.17	1.40
Elastic strength (V_e)	*	21100	70860	84700
Real strength (V_y)	*	20000	36200	38840
Corresponding strength for the start of nonlinear behaviour (V_s)	*	1762	1762	1762
Design strength (V_d)	*	26860	26860	26860
Response modification factor due to ductility (R_μ)	*	1.06	1.96	2.18
Response modification factor due to over strength (Ω_s)	*	1.13	2.05	2.2
Response modification factor due to allowable stress (R_d)	*	1	1	1
Response modification factor ($R = R_\mu.\Omega_s.R_d$)	3.5	1.2	4.02	4.81

Table 5: Demand and Supply R-Factors for the 24-Storey building under an artificial spectrum compatible accelerogram (R1)

Shear values are reported in (kN)	R Code	R Demand	R^1Supply	R^2Supply
Maximum ground acceleration (g)	0.35	0.35	0.95	1.1
Elastic strength (V_e)	*	34020	99300	115100
Real strength (V_y)	*	29100	36700	42400
Corresponding strength for the start of nonlinear behaviour (V_s)	*	23110	23110	23110
Design strength (V_d)	*	35900	35900	35900
Response modification factor due to ductility (R_μ)	*	1.17	2.7	2.71
Response modification factor due to over strength (Ω_s)	*	1.26	1.6	1.84
Response modification factor due to allowable stress (R_d)	*	1	1	1
Response modification factor ($R = R_\mu.\Omega_s.R_d$)	3.5	1.47	4.3	4.98

Table 6: Demand and Supply R-Factors for the 32-Storey building under an artificial spectrum compatible accelerogram (R_1)

Shear values are reported in (kN)	R Code	R Demand	R^1Supply	R^2Supply
Maximum ground acceleration (g)	0.35	0.35	0.96	1.18
Elastic strength (V_e)	*	37200	101700	125100
Real strength (V_y)	*	31370	56200	57400
Corresponding strength for the start of nonlinear behaviour (V_s)	*	23400	23400	23400
Design strength (V_d)	*	45390	45390	45390
Response modification factor due to ductility (R_μ)	*	1.18	1.81	2.18
Response modification factor due to over strength (Ω_s)	*	1.34	2.40	2.45
Response modification factor due to allowable stress (R_d)	*	1	1	1
Response modification factor ($R = R_\mu.\Omega_s.R_d$)	3.5	1.59	4.34	5.35

For each ordered pair (PGA, R) in A_0 area, the diagonal members which provide the main lateral load-resisting system remain in their elastic domain, and hence will exhibit low axial strain values. Selection of an R factor ranging from demand to supply values corresponding to a certain damage level, will ensure the structure remains in the desired performance level for the intensity required to reach this level of performance. As an example, for each ordered pair (PGA, R) highlighted in A_1 area in Figure (11- a, b and c) and the grey zone shown in Figure (11-d), the structure is still able to offer sufficient capacity to resist against lateral loads. In this case, the axial strain induced in diagonal members would be less than the limit values corresponding to the performance level of life safety. Similarly, the same interpretation can be conducted for A_2 area and performance level of collapse prevention.

It can be seen in Figure 11 that the designed structures remained in levels higher than the life safety under both DBE and MCE hazard scenarios. This implies that selection of code-based R factor equal to 3.5 for preliminary design of these systems could ensure the safety and stability of

the diagrid structures under both DBE and MCE hazard levels without posing significant damage. This conclusion is in agreement with the results presented in Figure (7).

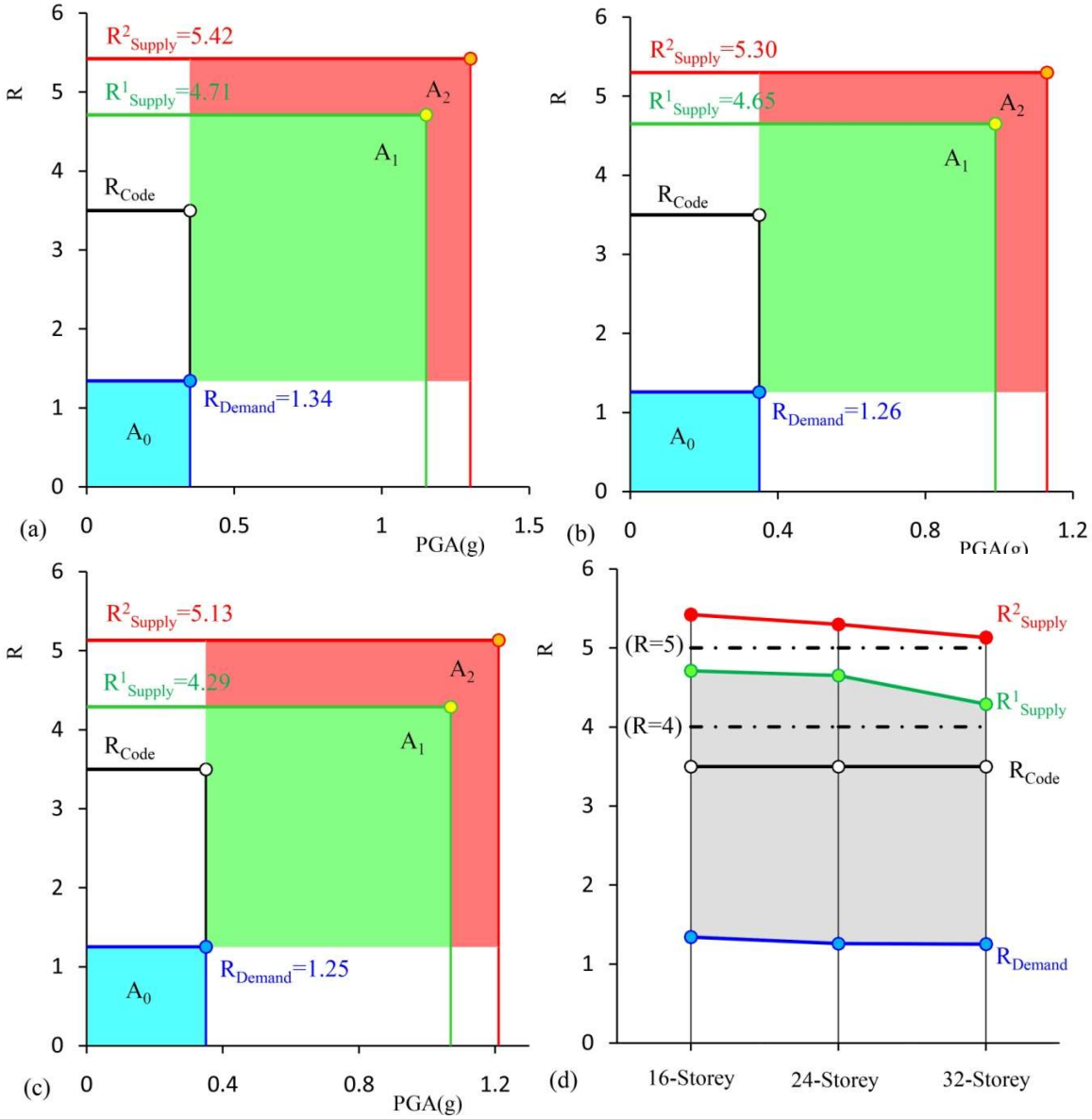

Fig (11): Comparison of Demand, Supply and Code-Based Response Modification Factors for (a) 16-storey, (b) 24-storey, (c) 32-Storey Building, and (d) Variations of R-factor versus height; Average of the results for R_1 to R_{12}

Using the proposed approach, response modification factors can be selected depending on the desired intensity and acceptable damage levels. In general, it can be noted from Figure (11-d) that as the building's height increases, the safety of the diagrid system is slightly decreased due to a

small increase in the demand and supply response modification factors. However, the results indicate that in case of DBE hazard level, the structures still provide an acceptable safety margin for modification factor of 4. This value of modification factor generally guarantees the performance levels higher than life safety under MCE hazard level as well. In case the response modification factor of 5 is used in the design process, at both DBE and MCE hazard levels the structures will remain at a performance level higher than collapse prevention. Considering the above information and the insignificant difference between R^1_{Supply} and R^2_{Supply}, the design modification factor of 4 is recommended for diagrid systems. These results are in agreement with the response modification factors proposed by Asadi and Adeli [12] and Heshmati and Aghakouchak [13]. It should be noted that the response modification factors proposed in this study are based on the selected diagrid systems and design assumptions, and therefore, may be affected by changing in the diagonals angle. This will be a topic of further investigation in future studies.

7. Summary and Conclusions

Although diagrid systems are increasing used as an efficient lateral load resisting system for tall buildings in modern construction, current literature lacks detailed information regarding their structural performance and appropriate seismic design parameters to ensure their reliability under different earthquake intensity events. To bridge this knowledge gap, this study aimed to assess the seismic reliability of diagrid structural systems and develop more efficient design methodologies. The demand and supply response modification factors were calculated for 16, 24 and 32-storey buildings with diagrid structural system designed in compliance with current standards under a set of 12 spectrum compatible earthquakes. The results of the reliability analyses were then used to develop a novel multi-level response modification factor (R-Factor) as a function of site seismicity and acceptable damage level. Based on the results presented in this paper, the following conclusions can be drawn:

1- It was shown that due to higher mode contributions, especially in tall diagrid systems, the analyses methods based on triangular or first mode lateral load distributions are not suitable for the preliminary design of such systems. Force and displacement responses were found to be sensitive to the intensity of the input excitation. Under the intensity levels corresponding to

DBE and MCE hazard levels, the top diagrid module exhibited higher drift ratios compared to the other storeys.

2- Similar maximum storey drifts were observed in the elastic and inelastic models subjected to DBE hazard level (PGA=0.35g). This indicates that under this level of intensity, the diagrid structures did not considerably exceed their elastic range.

3- Due to their considerable stiffness and redundancy, diagrid systems naturally benefit from a satisfactory seismic performance. The ratio of the maximum axial strain in diagonal elements to the strain corresponding to the critical buckling load under DBE and MCE events, indicates that under both hazard levels the diagrid buildings exhibit performance levels higher than life safety (LS) with around 99% reliability.

4- The capacity response modification factors corresponding to DBE hazard level were greater than the demand values in all the selected diagrid systems. Therefore, for preliminary design purposes it sufficient to use the code-based response modification factor equal to 3.5 and overstrength factor of 1.5 to ensure structural safety under DBE hazard level without developing significant damage in the main lateral load-resisting elements.

5- It was found that using a response modification factor equal to 4 for diagrid systems can maintain their acceptable safety margin to satisfy life safety performance level under DBE events. This value of response modification factor generally guarantees the performance levels higher than life safety for MCE hazard level as well.

In general, the results of this study demonstrated the good seismic performance and reliability of diagrid systems as a cost-effective alternative to conventional lateral load resisting systems in tall buildings. The proposed multi-level response modification factor should also prove useful in performance-based design of diagrid structural systems in seismic regions.

References

1. J. Khushbu, P. Patel, Analysis and Design of Diagrid Structural System for High Rise Steel Buildings. Procedia Engineering 51 (2013) 92-100.
2. I. Hajirasouliha, K. Pilakoutas K, General Seismic Load Distribution for Optimum Performance-Based Design of Shear-Buildings. Journal of Earthquake Engineering 16(2012) 443-462.

3. K. Moon, J.J. Connor, J.E. Fernandez, Diagrid Structural Systems for Tall Buildings: Characteristics and Methodology for Preliminary Design. The Structural Design of Tall and Special Buildings 16 (2017) 205-230.
4. C. Liu, Q. Li, Z. Lu, H. Wu, A review of the diagrid structural system for tall buildings. The Structural Design of Tall and Special Buildings 27(2018) 1:10.
5. J. Kim, Y.H. Lee, Seismic Performance Evaluation of Diagrid System Buildings. The Structural Design of Tall and Special Buildings 21 (2012) 736-749.
6. E. Mele, M. Toreno, G. Brandonisio, A. De Luca, Diagrid Structures for Tall Buildings: Case Studies and Design Considerations. The Structural Design of Tall and Special Buildings 23 (2014) 124-145.
7. K.S. Moon, Diagrid Structures for Complex-Shaped Tall Buildings. Procedia Engineering 12 (2011) 1343-1350.
8. E. Asadi, H. Adeli, Diagrid an innovative, sustainable, and efficient structural system. Structural Design Tall Special Buildings 26 (2017) 1-18.
9. E. Asadi, H. Adeli, Nonlinear behavior and design of mid-to-high-rise diagrid structures in seismic regions. Engineering Journal (American Institute of Steel Construction), 55(2018), 161-180.
10. E. Asadi, A. M.Salman., Y. Li, Multi-Criteria Decision-Making for Seismic Resilience and Sustainability Assessment of Diagrid Buildings, Engineering Structures 191(2019) 229-246.
11. E. Asadi, Y. Li, Y. Heo, Seismic Performance Assessment and Loss Estimation of Steel Diagrid Structures, Journal of Structural Engineering, 144(2018).
12. G. Lacidogna, D. Scaramozzino, A. Carpinteri, A matrix-based method for the structural analysis of diagrid systems, Engineering Structures 193 (2019) 340.
13. F. Zhao, C.H. Zhang, Diagonal Arrangements of Diagrid Tube Structures for Preliminary Design. The Structural Design of Tall and Special Buildings 24 (2015) 159-175.
14. C.H. Zhang, F. Zhao, Y. Liu, Diagrid Tube Structures Composed of Straight Diagonals With Gradually Varying Angles. The Structural Design of Tall and Special Buildings 21 (2012) 283-295.
15. G.M. Montuori, E. Mele, G. Brandonisio, A. De Luca, Design Criteria for Diagrid Tall Buildings: Stiffness Versus Strength. The Structural Design of Tall and Special Buildings (2013 1294-1314.
16. K. Moon, Optimal Grid Geometry of Diagrid Structures for Tall Buildings. Architectural Science Review 51 (2008) 239-251.
17. V. Tomei, M. Imbimbo, E. Mele, Optimization of structural patterns for tall buildings: The case of diagrid. Engineering Structures171 (2018) 280-297.
18. E. Asadi, H. Adeli, Seismic performance factors for low-to mid-rise steel diagrid structural systems. The Structural Design of Tall and Special Buildings 27 (2018) 1-18.

19. M. Heshmati, A.A. Aghakouchak, Quantification of seismic performance factors of steel diagrid system. The Structural Design of Tall and Special Buildings 28 (2019) 1-14.
20. FEMA P695, Quantification of Building Seismic Performance Factors, Federal Emergency Management Agency, Washington, 2009.
21. C.H. Huang, X. Han, J. Ji, J. Tang, Behaviour of Concrete-Filled Steel Tubular Planar Intersecting Connections Under Axial Compression, Part 1: Experimental Study. Journal of Engineering Structures 32 (2010) 60–68.
22. Y.J. Kim, I.Y. Jung, Y.K. Ju, S.J. Park, S.D. Kim, Cyclic Behaviour of Diagrid Nodes with H-Section Braces. Journal of Structural Engineering 136 (2010) 1111–22.
23. Y.J. Kim, M.H. Kim, I.Y. Jung, Y.K. Ju, S.D. Kim, Experimental Investigation of the Cyclic Behaviour of Nodes in Diagrid Structures. Journal of Engineering Structures 33 (2011) 2134–44.
24. I.Y. Jung, Y.J. Kim, Y.K. Ju, S.D. Kim, S.J. Kim, Experimental Investigation of Web-Continuous Diagrid Nodes Under Cyclic Load. Journal of Engineering Structures 69 (2014) 90–101.
25. Q. Shi, F. Zhang, Simplified calculation of shear lag effect for high-rise diagrid tube structure. Journal of Building Engineering 22 (2019) 486-495.
26. N. Mashhadiali, A. Kheyroddin, R. Zahiri, Dynamic Increase Factor for Investigation of Progressive Collapse Potential in Tall Tube-Type Buildings. Journal of Performance of Constructed Facilities 30 (2016) 365-374.
27. J. Kim, J. Kong, Progressive Collapse Behaviour of Rotor-Type Diagrid Buildings. The Structural Design of Tall and Special Buildings 22 (2013) 1199-1214.
28. Permanent Committee for Revising the Standard 2800, Iranian Code of Practice for Seismic Resistant Design of Buildings, 4th Edition, Building and Housing Research Center, Tehran, Iran, 2014.
29. ASCE/SEI 7-10, Minimum Design Loads and Associated Criteria for Buildings and Other Structures, American Society of Civil Engineers, Reston, Virginia, 2010.
30. ANSI/AISC 360-10, Specification for Structural Steel Buildings, American Institute of Steel Construction, Inc, Chicago, IL, 2010.
31. Computers and Structures Inc. (CSI), Structural and Earthquake Engineering Software, ETABS, Extended Three Dimensional Analysis of Building Systems Nonlinear Version 15.2.2, Berkeley, CA, USA, 2015
32. W. Baker, C. Besjak, M. Sarkisian, P. Lee, Ch. Doo, Proposed Methodology to Determine Seismic Performance Factor for Steel Diagrid Framed Systems. In: Council on Tall Buildings and Urban Habitat. City: Hawaii, 2010.

33. R. Liptack, Motion Based Seismic Design and Loss Estimation of Diagrid Structures, Thesis (MS) in Department of Civil and Environmental Engineering. Massachusetts Institute of Technology, 2013.
34. ANSI/AISC 341-10, American Institute of Steel Construction. Chicago, IL., 2010.
35. DIN 1025. Hot rolled I and H sections: dimensions, mass and static parameters. Berlin: DIN Deutsches Institut Fur Normung EV; 1995.
36. Computers and Structures Inc. (CSI), Structural and Earthquake Engineering Software, PERFORM-3D Nonlinear Analysis and Performance Assessment for 3-D Structures, Version 6.0.0, Berkeley, CA, USA, 2016.
37. ASCE/SEI41-17, Seismic Rehabilitation of Existing Buildings, American Society of Civil Engineers, 2017.
38. J. Hancock, J. Watson-Lamprey, N.A. Abrahamson, J.J. Bommer, A. Markatis, E. McCoy, R. Mendis, An improved method of matching response spectra of recorded earthquake ground motion using wavelets, Journal of Earthquake Engineering 10 (2006) 67-89.
39. PEER Ground Motion Database, Pacific Earthquake Engineering Research Center, Web Site: http:// peer.berkeley.edu/peer-ground-motion-database (accessed 10 Feb 2019)
40. F. Zareian, H. Krawinkler, L. Ibarra, D. Lignos, Basic Concepts and Performance Measures in Prediction of Collapse of Buildings Under Earthquake Ground Motions, The Structural Design of Tall and Special Buildings 19 (2010) 167-181.
41. V. Mohsenian, A. Mortezaei, Evaluation of seismic reliability and multi level response reduction factor (R factor) for eccentric braced frames with vertical links, Earthquakes and Structures 14 (2018) 537-549.
42. V.V. Bertero, Evaluation of response reduction factors recommended by ATC and SEAOC. Proc.3rd U.S.Nat1 Conf. on Earthquake Engineering, South Carolina: 1663-1670, 1989.
43. A. Whittaker, G. Hart, C. Rojahn, Seismic response modification factors, Journal of structural Engineering 125 (1999) 438-444.
44. S.P. Lia, J.M. Biggs, Inelastic response spectra for seismic building design. Journal of the Structural Division 106 (1980) 1295-1310.
45. E. Miranda E, Seismic evaluation & upgrading of existing buildings, A PhD Thesis, University of California at Berkeley, 1991.
46. ATC-19 Report, Structural Response Modification Factors, Applied Technology Council, Redwood City, California, 1995.
47. H. Moghaddam, R. KaramiMohammadi, Ductility reduction factor of MDOF shear-building structures, Journal of structural Engineering 5 (2001) 425-440.
48. P.A. Santa-Ana, Estimation of strength reduction factors for elastoplastic structures: Modification factors. 13th World Conference on Earthquake Engineering, Vancouver, Canada, Paper No. 126, 2004.

49. A.S. Elnashai, A.M. Mwafy, Over strength and force reduction factors of multi storey reinforced concrete buildings. The Structural Design of Tall Buildings 11 (2002) 329-351.
50. N. Fanaie, E. Afsar Dizaj, Response modification factor of the frames braced with reduced yielding segment BRB. Structural Engineering and Mechanics 50(2014) 1-17.
51. D. Brahmavrathan, C. Arunkumar, Evaluation of response reduction factor of irregular reinforced concrete framed structures. Indian Journal of Science and Technology, 9 (2016) 1-8.
52. A.M. Mwafy, A.S. Elnashai, Calibration of force reduction factors of RC buildings. Journal of Earthquake Engineering 6 (2002) 239-273.